Theoretical characterization of alumina and sulfated-alumina catalysts for *n*-butene isomerization

María Luján Ferreira[a], Elsa Haydeé Rueda[b],*

[a] *PLAPIQUI (UNS-CONICET) Camino La Carrindanga, km 7, CC 717, 8000 Bahía Blanca, Argentina*
[b] *Departamento de Química e Ingeniería Química, Universidad Nacional del Sur Avda. Alem 1253, 8000 Bahía Blanca, Argentina*

Abstract

A theoretical study was carried out in order to characterize the changes produced by the presence of sulfate on the alumina surface. A molecular orbital approach of the extended Hückel (EH) type together with dynamic molecular calculation were performed to evaluate adsorption and desorption energies of the intermediate species for skeletal and double-bond isomerization reactions of *n*-butene The bimolecular and monomolecular mechanisms for skeletal isomerization were evaluated. © 2002 Elsevier Science B.V. All rights reserved.

1. Introduction

Isomerization reactions involving double-bond *n*-butene isomerization and skeletal *n*-butene isomerization were profusely investigated [1–10]. Double-bond isomerization of *n*-butene is described in more details in relation to the acid–bases properties of catalysts. The rate usually increases either increasing acid strength and acid amount or increasing base strength and base amount [11–13]. An apparent correlation exists between selectivity and acidity or basicity of catalysts [2].

Over Brønsted solid acids, the intermediate is a sec-butyl cation formed by the addition of a proton from the solid surface to butene. The same intermediate is often involved in the case of Lewis solid acids. In the latter case, protonic acid is induced by reac-

tion of the butene on the Lewis acid site. The variation in the rate and the selectivity found on increasing acid strength can be explained considering the linear free energy relationships and the stability of sec-butyl cation in the kinetics data. Rate of isomerization is highly accelerated if alkyl groups are substituted at the carbocation center because the carbocation is stable in the order tertiary > secondary > primary [2].

The *cis/trans* ratio from 1-butene is usually very large in the case of solid bases. This is because the allyl intermediate formed by the abstraction of proton from butene is more stable in the *anti* form than in the *syn* form [2].

Skeletal isomerization of *n*-butene is preferably described through an unimolecular pathway. The best catalysts for *n*-butene skeletal isomerization are found among the oxides. However, an exhaustive research of Cheng and Ponec [3] showed that only a few single-cation oxides such as W-, Mo-, and Al-oxides, are really promising. The surface of the mentioned oxides expose the Lewis acidic (LA) sites, the Lewis

* Corresponding author.
E-mail addresses: mlferreira@plapiqui.edu.ar (M.L. Ferreira),
ehrueda@criba.edu.ar (E.H. Rueda).

basic (LB) sites and Brønsted acidic (BA) sites, possibly associated with LA sites. Hounvicka et al. [8] suggest that Brønsted acidic sites of moderate acidity are the active sites in skeletal isomerization.

Since parameters of catalytic reactions as *n*-butene pressure and temperature differ for isobutene and for by-products formation [6,8,14,15], the isobutene and by-products (mainly C_3 and C_5) must be formed by different mechanisms and on different sites [8]. In both cases, BA sites are active, but their acidity strengths are different. The presence of very strongly acidic BA sites induces excessive by-products formation [16]. Thus, the selectivity of a catalyst is low if strong Brønsted acid sites are present.

The alumina is inactive as a catalyst for the cracking of hydrocarbons because its Brønsted acid sites are too weak. In order to achieve an increment in the acidic properties of alumina, several researches [6,16–33], treated this oxide with different anions.

Arata and Hino [23,34] found in the case of γ-Al_2O_3, that highly active catalysts were obtained by sulfate addition on the crystallized oxide rather than the amorphous one. Pryzystajko et al. [19] compared sulfated-alumina with pure alumina and concluded that the sulfate enhances the acidic and oxidizing properties but diminishes the basic and reducing properties. Enhanced acidity in sulfated-alumina is attributed to protonation of surface OH groups with the appearance of strong Brønsted acidity. Such acidity is absent in pure alumina. The catalytic behavior of the sulfated-alumina in many aspects is similar to those exhibited by silica–alumina and by fluorinated-alumina.

In this work, a molecular orbital study of the extended Hückel (EH) type has been carried out for pure alumina and sulfated-alumina. We also performed a simple molecular dynamics calculation, in order to evaluate the temperature effect over the behavior of the intermediates adsorbed on alumina surface, sec- and tert-butyl cations. By the light of these results, the optimal conditions for both are discussed.

2. Theoretical methods

2.1. Extended Hückel modified method (EHMO)

The semi-empirical EH method [35] has been extensively applied to study of the electronic structure

Table 1
Extended Hückel parameters

Atom	Orbital	Ionization potential (eV)	Orbital exponents
H	1s	−13.60	1.00
O	2s	−31.60	2.163
	2p	−16.78	2.750
C	2s	1.154	−19.65
	2p	1.451	−11.13
Al	3s	−12.30	1.670
	3p	−6.50	1.383
S	3s	−20.00	1.220
	3p	−11.00	1.827

of molecules. In the present work, we have employed a modified version of this method, ICONC, developed by Calzaferri et al. [36]. Although this method does not calculate representative absolute energies, it can be employed to predict qualitative trends in model system. ICONC has been applied to study the CH_3OH adsorption–oxidation process on V_2O_5 [37] and to the analysis of Ferreira et al. [38] and VO_x/γ-Al_2O_3 catalyst [37]. Table 1 shows the used parameters in the EHMO calculation.

The EHMO was widely used by Hofmann [35] to study electronic structure of transition metal complexes and adsorbed molecules; it provides useful qualitative trends in large model system. The electronic structure and derived properties are established from electron equations for the molecular orbitals, approximated by experimental data. In this formalism, the non-diagonal elements of the Hamiltonian of the system are proportional to the overlap matrix elements. In order to improve the traditional extended Hückel–Hamiltonian, some corrections were introduced by Yamaguchi et al. [21].

The total energy of a selected species is a sum over of an attractive and a repulsive term and may be represented by the following equation:

$$E_t = \sum_i n_i E_i + \frac{1}{2} \sum_{\substack{i,j \\ i \neq j}} E_{\text{rep}(i,j)}$$

The attractive energy is related to the electrons in the valence level i with an occupancy n_i. The repulsion energy is originated between all the possible pairs nucleus i–fixed atom j.

Experimental parameters are necessary for calculations, being the EHMO a semi-empirical method. We have used reported ionization potential obtained from spectroscopic data. Since for the level 4p only theoretical data are available in literature, we have taken the data of Hartree–Fock–Slater. For more details, please look [37–39].

The energies were calculated for all the involved species in a reaction. The relative energy (reported as ΔE) is the energetic difference between products and reactants for each reaction.

2.2. Modeling of γ-Al₂O₃

The cluster approach was applied to approximate the study of the real support. γ-Al₂O₃ was modeled as a portion of the infinite solid. An undesirable effect appears in the system, the so-called dangling bond; hydrogen atoms were used to complete the internal aluminum coordination. Another disadvantage is the importance of the missing atoms in determining the electric field at the surface. However, we have considered that a two-layer alumina cluster is adequate

for modeling a support crystal based on the theoretical work of Pisani et al. [39]. These authors have performed Hartree–Fock characterization of Al_2O_3 and they have concluded that a two-layer cluster is adequate for modeling an ionic crystal surface.

The model of γ-Al_2O_3 was constructed based on a tetragonal-distorted defect spinel structure [40,41], with aluminum cations arranged in an approximately cubic close-packed oxygen array. We have considered that the preferentially exposed planes are (1 0 0) and faces C and D of the (1 1 0) plane (Figs. 1–3) [41,42]. Undoubtedly, other planes such as (1 1 1) may exist but they are less abundant. Therefore, they are not considered in the present model.

The number of aluminum, oxygen and hydrogen atoms for each cluster analyzed in our study is reported in Table 2. The surfaces with defects include a minor amount of atoms.

2.3. Modeling of γ-Al₂O₃ surfaces with defects

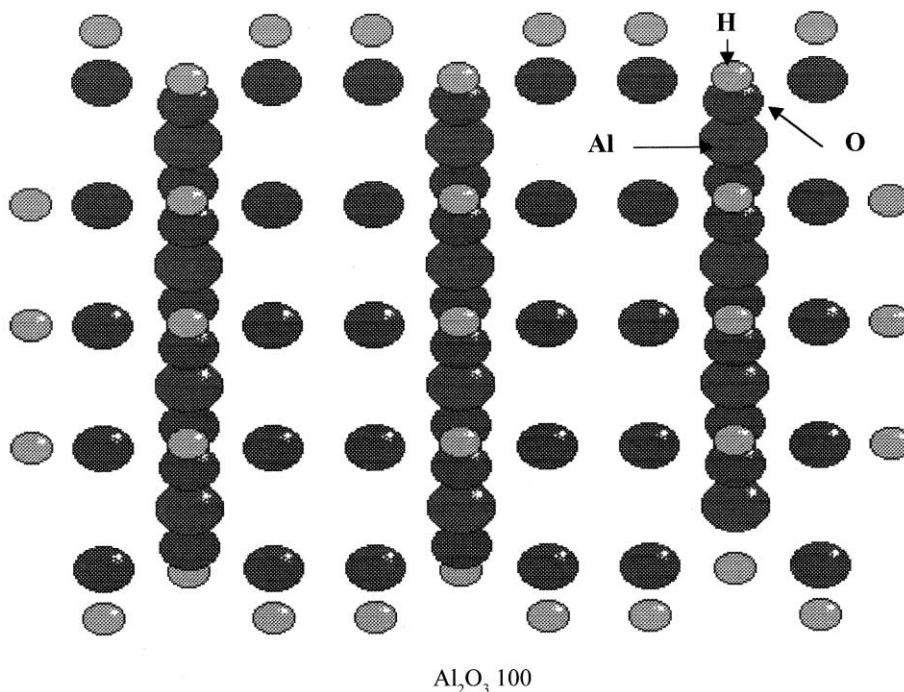To take into account the effects of thermal pretreatment on the alumina structure, several defects were
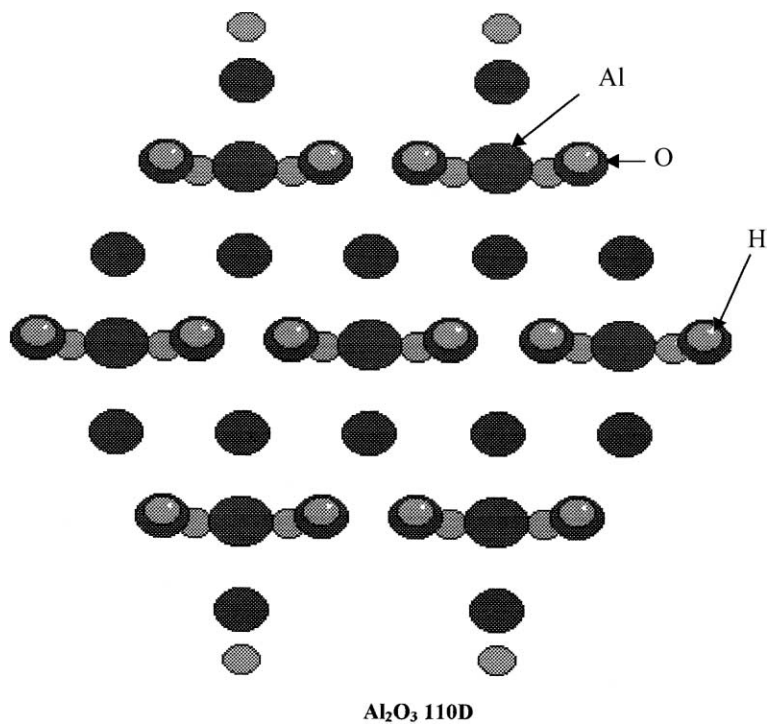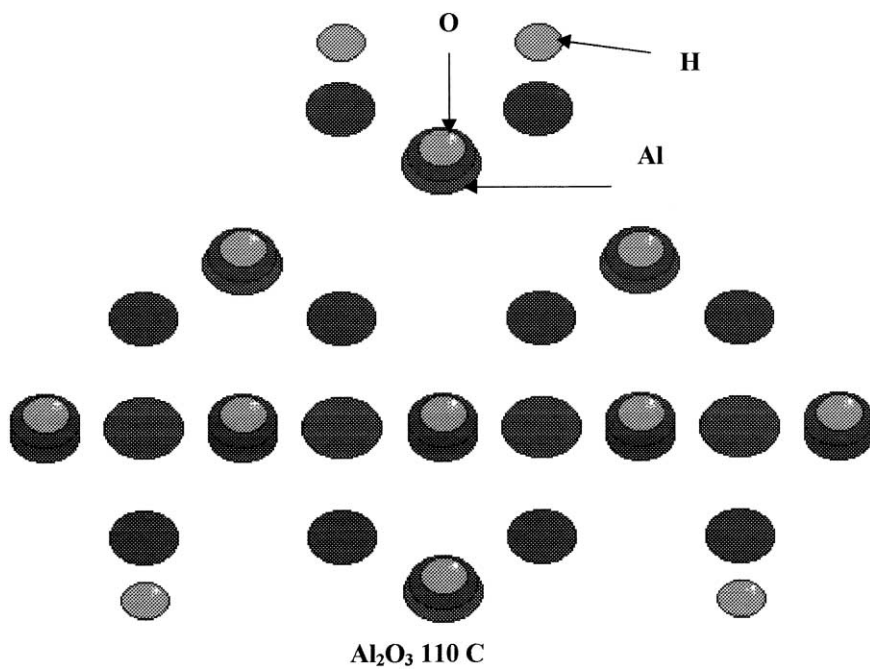

Fig. 1. (1 0 0) plane of γ-Al₂O₃.

Fig. 2. (1 1 0)D plane of γ-Al_2O_3.

Fig. 3. (1 1 0)C plane of γ-Al_2O_3.

Table 2
Number of Al, O and H atoms in different complete faces of γ-Al$_2$O$_3$

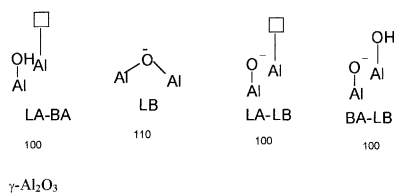| Plane	Number of O atoms	Number of Al atoms	Number of H atoms
(1 0 0)	53	12	46
(1 1 0)C	24	8	19
(1 1 0)D	28	7	42

Fig. 4. Defective sites considered in γ-Al$_2$O$_3$.

modeled on the three different planes. These defects are one-pairs LA–BA and two LB sites and combinations mainly placed in planes (1 0 0) and (1 1 0)C (Fig. 4).

2.4. Modeling of $SO_4{}^{2-}/\gamma$-Al_2O_3 surfaces

$SO_4{}^{2-}/\gamma$-Al$_2$O$_3$ was modeled taking into account two different reactions and final structures.

1. Reaction with the complete surface for the three planes to generate a dioxo species (Scheme 1-Reaction 1).
2. Reaction with surface structural defects for the three planes to generate a monoxo species (Scheme 2-Reaction 2).
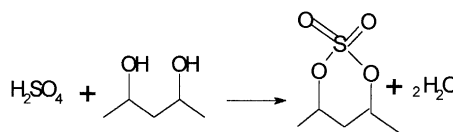
Scheme 1-Reaction 1.
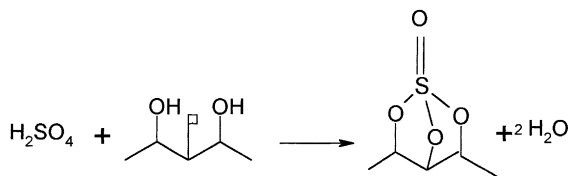
Scheme 2-Reaction 2.

In the case of the reaction 2, we considered a surface with a Lewis acid site.

Table 3 shows the results of reactions 1 and 2 on the three selected planes.

2.5. Modeling of butenes

The butenes were modeled with all its atoms and taking into consideration the relevant facts about their structures. Carbocations were modeled by one-electron loss, and carbanions by one-electron gain.

2.6. Molecular dynamics calculation-MM2

To get some insight in the behavior of the adsorbed sec- and tert-butyl forms on alumina surface with the increase of temperature, we performed molecular dynamics calculation using the Chem 3D 5.0

Table 3
Formation energy of different supported SO$_x$ species

Plane	Final structure	Reaction	Formation energy (eV)
Al$_2$O$_3$(1 0 0)	SO$_4$–Al$_2$O$_3$(1 0 0)	1	−9.05
Al$_2$O$_3$(1 1 0)C	SO$_4$–Al$_2$O$_3$(1 1 0)C	1	−9.15
Al$_2$O$_3$(1 1 0)D	SO$_4$–Al$_2$O$_3$(1 1 0)D	1	−8.03
Al$_2$O$_3$(1 0 0) with LA	SO$_4$–Al$_2$O$_3$(1 0 0)	2	−12.30
Al$_2$O$_3$(1 1 0)C with LA	SO$_4$–Al$_2$O$_3$(1 1 0)C	2	−34.22
Al$_2$O$_3$(1 1 0)D with LA	SO$_4$–Al$_2$O$_3$(1 1 0)D	2	−7.27

(Cambridge Soft). Molecular dynamics and molecular mechanics could provide important arguments for the understanding of stability and selectivity of the adsorbed intermediate species [43]. A simple model of sec- and tert-butyl fragments attached to a model ($Al_3O_7H_4$) is maintained fixed, the alumina surface model is fixed immobile during this calculation. Only the directly attached Al–O bond is considered in the calculation. We performed the molecular dynamics calculation at several target temperatures. The step interval was set at 2 fs, the heating/cooling rate was 4.18 kJ per atom ps and the calculation finished after 10,000 steps. The procedure of calculation is an initial MM2 minimization proce-

dure (using Chem 3D 5.0) and later the MD calculation.

3. Results and discussion

3.1. Structures of $SO_4{}^{2-}/\gamma$-Al_2O_3

From the theoretical calculation results, the more abundant SO_x species are from reaction 2 on planes (1 1 0)C and (1 0 0) and from reaction 1 for γ-Al_2O_3(1 1 0)C (see Table 3). These species are important when the concentration of LA–BA sites is important. For a highly hydroxylated
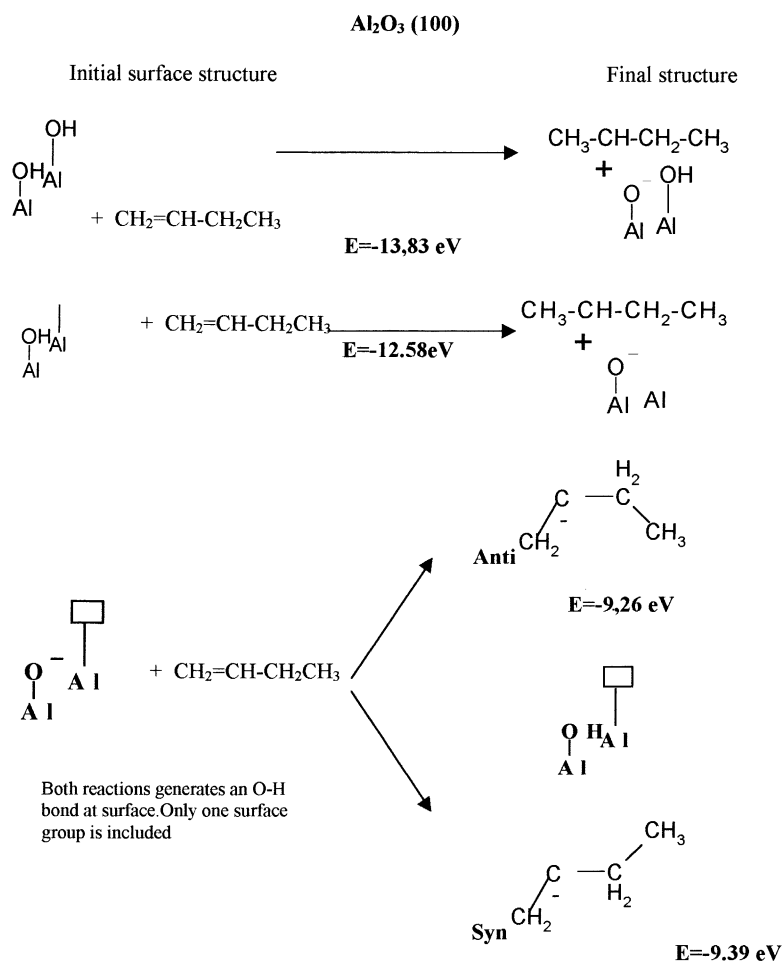

Fig. 5. Surface structure of butene adsorbed on (1 0 0) plane of γ-Al_2O_3.

support, the dioxosulfur species would be predominant.

3.2. Modeling of 1-butene adsorption-reaction with surface

The steps considered at this point are as follows:

1. The sec-butyl carbonium formation, by reaction with a Brønsted acidic site.
2. The *anti-* and *syn*-carbanion formation, by reaction with a Lewis basic site (for double-bond isomerization).

Figs. 5 and 6 show the results for the different surfaces considered. We considered the planes (1 0 0) and (1 1 0)C of γ-Al$_2$O$_3$, because the results of EHMO calculation say that these both planes are the most important for 1-butene reactions. The energy reported as

Table 4
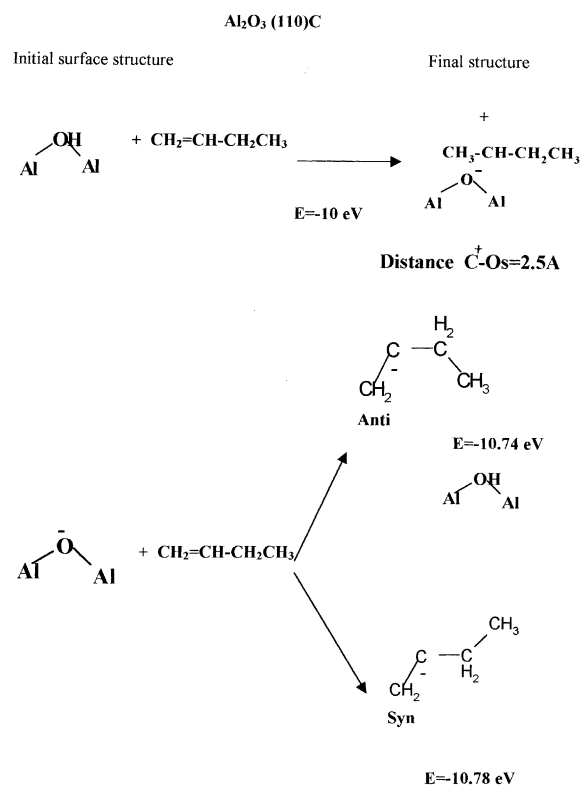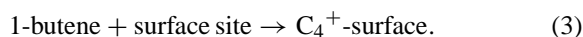Sec-butyl carbocation formation on an OH near a SO$_x$ group

Surface	Surface	Reaction formation energy of C$_4^+$-surface (eV)
SO$_4$–Al$_2$O$_3$(1 0 0)	1	−13.63
SO$_4$–Al$_2$O$_3$(1 1 0)C	1	−27.77
SO$_4$–Al$_2$O$_3$(1 1 0)D	1	−2.86
SO$_4$–Al$_2$O$_3$(1 0 0)	2	−12.5
SO$_4$–Al$_2$O$_3$(1 1 0)C	2	−4.98
SO$_4$–Al$_2$O$_3$(1 1 0)D	2	−3.26

reaction energy is the energy for the reaction

$$1\text{-butene} + \text{surface site} \rightarrow C_4^+\text{-surface}. \qquad (3)$$

Only a fraction of the surface is depicted in the figures. The calculation was taking into account the complete structure of the plane.

The final structure can be charged (carbonium or carbanion) or not. The method (EHMO) cannot evaluate the strength of the OH considered. It is known than γ-Al$_2$O$_3$ has no high Brønsted acidity when it is pretreated at low temperatures. The strength of the OH changes because changes in the frame of the support take place by thermal treatment, or introduction of some anionic groups.

Table 4 shows the results obtained for the reaction of sec-butyl carbonium formation near different SO$_4^{-2}$ groups.

3.3. Modeling of isomerization of 1-butene to cis–trans-2-butene

This double-bond isomerization is considered to take place through a carbanionic or through a carbocationic mechanism, therefore, we considered both possibilities. Basic and acidic sites are possible active sites for double-bond isomerization.

On Brønsted acid sites, the formation of a sec-butyl cation is the needed step and later the desorption of *cis-* or *trans-*2-butene. On Lewis basic sites, the abstraction of H$^+$ from 1-butene gives two possibilities: the formation of *anti* (precursor of *cis*) or *syn* (precursor of *trans*) carbanionic species on alumina surface, adsorbed through the formation of an allylic group (see Figs. 5 and 6). If the Brønsted sites are enough acidic,

Fig. 6. Surface structure of butene adsorbed on (1 1 0)C plane of γ-Al$_2$O$_3$.

Table 5
Isomerization of 1-butene to *cis–trans*-2-butene

Reaction		ΔE (eV)
4	*Anti*-Al$_2$O$_3$(1 0 0) + 1-butene → *cis*-2-butene + *anti*-Al$_2$O$_3$(1 0 0)	0.27
5	*Anti*-Al$_2$O$_3$(1 0 0) + 1-butene → *cis*-2-butene + *syn*-Al$_2$O$_3$(1 0 0)	0.13
6	*Syn*-Al$_2$O$_3$(1 0 0) + 1-butene → *trans*-2-butene + *syn*-Al$_2$O$_3$(1 0 0)	0.00
7	*Syn*-Al$_2$O$_3$(1 0 0) + 1-butene- → *trans*-2-butene + *anti*-Al$_2$O$_3$(1 0 0)	0.14

both mechanisms can be acting together, specially at low temperatures [6].

3.4. Modeling of skeletal isomerization of 1-butene to isobutene

The isomerization of 1-butene to isobutene is considered to take place in several steps. There are two mechanisms evaluated in open literature: monomolecular and bimolecular.

In the monomolecular mechanism, we considered several steps:

1. Formation of sec-butyl cation by reaction with a Brønsted reactive site (see Figs. 5 and 6 and Table 4).
2. Isomerization to tert-butyl cation.
3. Desorption of isobutene.

In the bimolecular mechanism, we considered that

1. An adsorbed carbonium is formed on surface in a first step.
2. Reaction of the adsorbed species with 1-butene from gas phase and formation of C$_8$$^+$ (methylheptane).
   2.1. Desorption of subproducts (pentene, propylene).
3. Isomerization to dimethylhexane.
   3.1. Desorption of isobutene and *cis–trans*-2-butene (even 1-butene unreacted).
4. Isomerization to trimethylpentane.
   4.1. Desorption of isobutene.

3.5. Modeling of reactive adsorption-product desorption

The reactions of adsorption–desorption are considered to be important because the adsorption is very strong in the case of carbenium ions.

3.6. Isomerization of 1-butene to cis–trans-2-butene

The desorption of *cis*- and *trans*-2-butene from (1 0 0) plane can be visualized through the reactions presented in Table 5 (reactions 4–7).

For the (1 1 0)C plane there is no difference in the formation energy for *syn*- and *anti*-adsorption forms.

It is clear that *cis*-2-butene formation would be preferred because of steric reasons when we considered the alternative mechanism shown in Fig. 7. In this figure, the presented results are from (1 1 0)C plane and the reactive olefin is 1-butene. Through an isomerization step, new forms of adsorption are claimed to
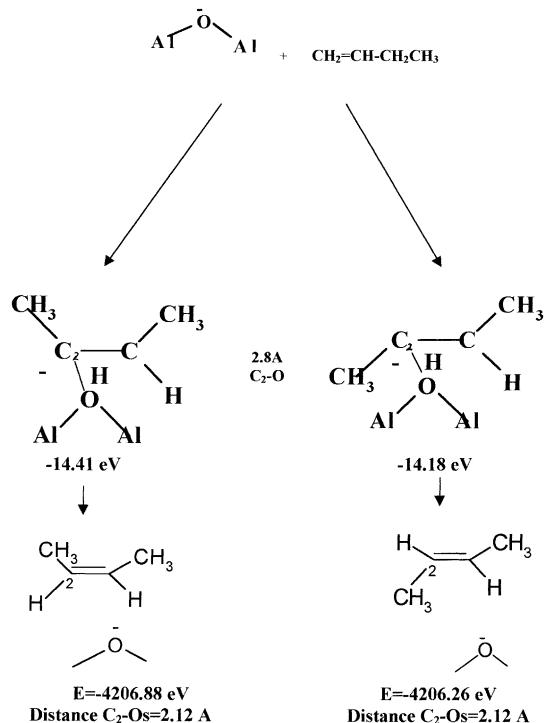

Fig. 7. *Cis/trans*-2-butene formation.

occur (compare Fig. 6 (*anti* and *syn* forms) and Fig. 7). The *anti* form in this case has the methyl groups of carbanion far away from the surface, whereas in Fig. 6, they are close to the surface. The energies change from −10.8 eV to near −14.4 eV. The distances are close to 3 Å in the case of the Fig. 7 and even minor when the olefin is formed (near 2.12 Å). Reordering of the surface structures of Fig. 6 by H migration from C_3 to C_1 produces the adsorbed species in Fig. 7. For the reactions of *cis*- and *trans*-2-butene adsorption on the basic site, the energy varies from −2.8 eV for *cis*- to −2.4 eV for *trans*-2-butene formation.

3.7. Skeletal isomerization-monomolecular mechanism

We analyzed the most important planes of γ-Al_2O_3. Table 6 presents the results from reactions 8 to 15. The relative adsorption energies of charged species are too much negative to consider desorption.

Desorption of isobutene is a difficult process from a monomolecular mechanism (reactions 10 and 11). It has been reported that at low temperatures, isobutene is not a product of 1-butene isomerization using not pretreated γ-Al_2O_3 [6]. Near a SO_x group the sec-butyl cation maintains its adsorption energy for (1 0 0) and (1 1 0)C planes, especially for OH near a SO_4 group from reaction 1. The adsorption energy is much higher for the (1 1 0)C plane (see Table 4) and cation adsorption near a SO_4 group. Adsorbed species obtained near a sulfate group from reaction 2 have lower adsorption energies. This fact is very important because the subsequent reactions for this precursor are affected. The adsorption would be strong if no high LA sites concentration was present, especially

for (1 1 0)C plane and near the dioxosulfur species (Table 4).

The formation of isobutene would be favored when SO_x is present on γ-Al_2O_3(1 0 0) plane, because the relative energy is similar to *cis*-2-butene formation. The steric interactions seem to play a role in these isomerizations (see reactions 12–15).

We must keep in mind that the alternative mechanism for double-bond isomerization is acting through the carbanion formation, besides this mechanism.

3.8. Bimolecular mechanism

To consider the skeletal isomerization of 1-butene, we analyzed the possibility of C_8^+ formation on alumina, through the dimerization of the adsorbed sec-butyl species. We need that the sec-butyl cation remains at surface enough time to react with butenes from gas phase to give a chance to the bimolecular mechanism to occur. The condition for this would be a high 1-butene concentration and strong C_4^+ adsorption, with no possibilities for the monomolecular mechanism to take place. It seems that SO_x species could be not favoring the bimolecular mechanism, taking into account the distribution of monoxosulfur and dioxosulfur species. If dioxosulfur species are present, the adsorption of C_4^+ is stronger than for the untreated support, but if the monoxosulfur species is at high concentration, the adsorption is weaker for the sec-butyl cation (see Table 4). In this sense, the initial thermal pretreatment of the support is very important to achieve one or the other situation.

Fig. 8 shows the formation of methylheptane, dimethylhexane or trimethylpentane by reaction of the sec-butyl cation with 1-butene on pure γ-Al_2O_3.

Table 6
Skeletal isomerization-monomolecular mechanism

| Reaction		ΔE (eV)
8	Sec-butyl cation–surface Al_2O_3(1 0 0) → tert-butyl cation–surface Al_2O_3(1 0 0)	−1.9
9	Sec-butyl cation–surface Al_2O_3(1 1 0)C → tert-butyl cation–surface Al_2O_3(1 1 0)C	−5.5
10	Tert-butyl cation–Al_2O_3(1 1 0)C + 1-butene → sec-butyl cation–Al_2O_3(1 1 0)C + isobutene	5.0
11	Tert-butyl cation–Al_2O_3(1 0 0) + 1-butene → sec-butyl cation–Al_2O_3(1 0 0) + isobutene	1.4
12	Sec-butyl cation–$SO_4Al_2O_3$(1 0 0) → tert-butyl cation–$SO_4Al_2O_3$(1 0 0)	−0.7
13	Tert-butyl cation–$SO_4Al_2O_3$(1 0 0) + 1-butene → sec-butyl cation–$SO_4Al_2O_3$(1 0 0) + isobutene	+0.21
14	Sec-butyl cation–Al_2O_3(1 1 0)C + 1-butene → sec-butyl cation–Al_2O_3(1 1 0)C + *cis–trans*-2-butene	0.0 (*trans*) 0.27 (*cis*)
15	Sec-butyl cation–Al_2O_3(1 0 0) + 1-butene → sec-butyl cation–Al_2O_3(1 0 0) + *cis–trans*-2-butene	0.0 (*trans*) 0.27 (*cis*)
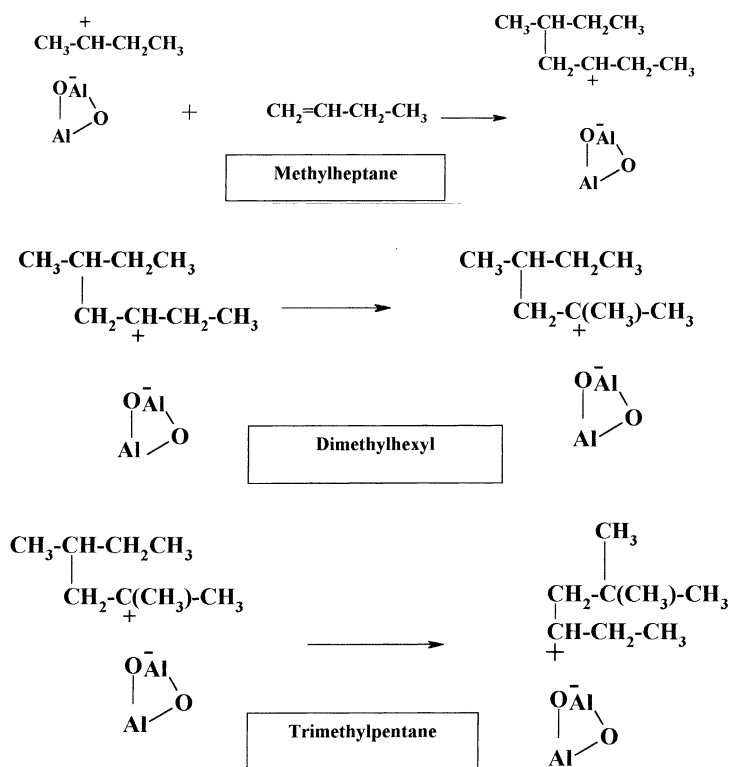
Fig. 8. Methylheptane formation and its isomerization to dimethylhexane and trimethylpentane.

From reactions 16 and 17, it is clear that the isomerization to dimethylhexyl cation is favored, whereas isomerization to trimethylpentyl cation is not. It is clear too, that high temperatures are needed to achieve the formation of this branched cation.

The formation of by-products by cracking of octenyl cations can be visualized by the reactions presented in Table 7 (see reactions 19–22).

The values for the desorption energies are positive and this fact is in agreement with the behavior of the treated alumina with the temperature in terms of reaction by-products of 1-butene isomerization. The deactivation is clearly understood looking at the high desorption-energies. We need high temperatures to desorb the reaction products and carbon formation surely takes place with these systems due to reactions

Table 7
Bimolecular mechanism

Reaction		ΔE (eV)
16	Sec-butyl cation–$Al_2O_3(1\,0\,0)$ + 1-butene → methylheptyl cation–$Al_2O_3(1\,0\,0)$	−7.64
17	Methylheptyl cation–$Al_2O_3(1\,0\,0)$ → dimethylhexyl cation–$Al_2O_3(1\,0\,0)$	−2.08
18	Dimethylhexyl cation–$Al_2O_3(1\,0\,0)$ → trimethylpentyl cation–$Al_2O_3(1\,0\,0)$	+1.35
19	Methylheptyl cation–$Al_2O_3(1\,0\,0)$ → propylene + isopentyl cation–$Al_2O_3(1\,0\,0)$	+4.37
20	Isopentyl cation–$Al_2O_3(1\,0\,0)$ + 1-butene → isopentene + sec-butyl cation–$Al_2O_3(1\,0\,0)$	+5.95
21	Dimethylhexyl cation–$Al_2O_3(1\,0\,0)$ + 1-butene → isobutene + sec-butyl cation–$Al_2O_3(1\,0\,0)$	+9.24
22	Sec-butyl cation–$Al_2O_3(1\,0\,0)$ + 1-butene → *cis–trans*-2-butene + sec-butyl cation–$Al_2O_3(1\,0\,0)$	0 (*trans*) 0.27 (*cis*)
23	Trimethylpentyl cation–$Al_2O_3(1\,0\,0)$ + 1-butene → isobutene + tert-butyl cation–$Al_2O_3(1\,0\,0)$	5.98
24	Tert-butyl cation–$Al_2O_3(1\,0\,0)$ + 1-butene → isobutene + sec-butyl cation–$Al_2O_3(1\,0\,0)$	0.5

Table 8
Molecular dynamics calculation—steric energy in kJ/mol[a]

	1	2	1	2	1	2	1	2	1	2
Final T (°C)	21 ± 42	62 ± 40	50 ± 48.4	62 ± 40	75 ± 48	112 ± 58	103 ± 50	112 ± 58	125 ± 48[b]	211 ± 63
Steric energy	377.9	379.1	405.0	379.1	416.3	430.5	446.4	430.5	472.3	535.0

[a] 1-Sec-butyl cation; 2-tert-butyl cation.
[b] The species is unstable.

Table 9
Molecular dynamics and MM2 calculation results[a]

	3	4	5	6
Final T (°C)	102 ± 33	104 ± 40	103 ± 30	101 ± 35
Steric energy (MD)	344.0	337.3	270.4	370.0
Steric energy (MM2)	13.8	4.6	−24.2	7.9

[a] 3-*Cis*-butene; 4-*trans*-butene; 5-isobutene; 6-1-butene.
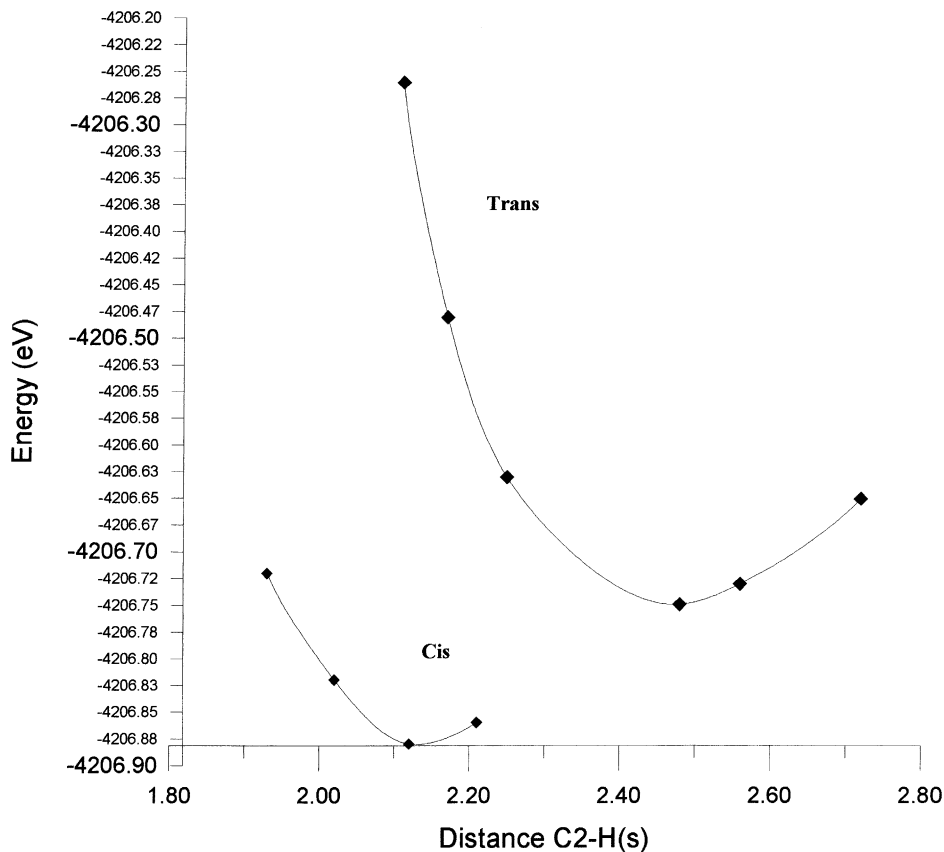

Fig. 9. Overall energy involved in *cis/trans*-2-butene adsorption.

of further dehydrogenation and oligomerization, reactions that are claimed to be responsible for the catalyst deactivation [2].

The interest in skeletal isomerization of butene has been extensively studied the last years because of two reasons: perhaps some day there could be excessive butene in the market and the need to keep a high octane Number in gasoline by methyl-tertiary-butyl-ether (MTBE). This product is produced from methanol and isobutene.

3.9. Molecular dynamics calculation-MM2

We reported the steric energies of the different supported-alcoxy species in Table 8.

It is clear from the Table 8 that the sec-butyl cation becomes unstable at temperatures lower than tert-butyl cation The tert-butyl cation needs temperatures about $232 \pm 64\,°C$ to achieve such unstable situation The calculations of the different situations of desorbed cis–trans-butene, 1-butene, and isobutene are presented in Table 9. The MD calculations were done considering the surface fixed (with $Al_3O_7H_5$) and the molecule of adsorbate, initially near to the surface. Only the movement of butene is considered in the calculation. The molecular dynamics computation consists of a series of steps which occur at a fixed interval ($2–1\,fs$, $1 \times 10^{-15} = 1\,fs$). The Beeman algorithm for integrating the equations of motion with improved coefficients is used to compute new positions and velocities of each atom at each step.

The results of Table 9 allow us to say that the most probable desorbed species is claimed to be isobutene, if tert-butyl cation is formed. In the case of sec-butyl cation, trans-butene would be slightly favored by $6.7\,kJ/mol$. When the molecule is considered alone in the MM2 calculation, the difference is $9.2\,kJ/mol$. In terms of steric energy, the order of stability of the butenes, considered without the surface, would be, isobutene > trans-butene > 1-butene > cis-butene. The fact that, at low temperatures, the cis/trans ratio is higher than 1.5 [9] can be related to the fact that the mechanism that takes place in this case is through LB sites. Fig. 7 shows the formation of an intermediate in the cis/trans reaction, after the anti–syn forms. It is clear that the cis-2-butene is preferred to trans-2-butene due to steric reasons. This situation is

clear when we compare the overall energy and this can be observed in Fig. 9.

4. General discussion

From the revised open literature of the last years [7], the following conclusions can be obtained:

1. Brønsted acid sites are required for skeletal isomerization of butene.
2. Their acidity needs not to be very strong.
3. The Lewis acid sites might play some minor role, but they are not the most essential sites.
4. The presence of very strong Brønsted acid sites induces by-product formation.
5. An increase of 1-butene pressure leads to a decrease in the isobutene yield, whereas an increase in the reaction temperature has an opposite effect. Two conclusions are obtained from these facts:
   5.1. Dimerization is responsible for the by-products formation.
   5.2. The main mechanism of isobutene formation is monomolecular.
6. Two main groups of by-products can be discerned: isobutane on one hand and propenes with pentenes on the other. This theoretical fact correlates well with experimental data.
7. Restriction of the space around the active center is efficient in suppress the side reactions and catalyst deactivation.
8. The double-bond isomerization is altered using sulfated-alumina, comparing it to alumina. Pryzstajko et al. [19] suggest that the reduction of basic sites is more prevalent on the surface of pure alumina.

We found a correlation between theoretical results and all these experimental facts.

1. The formation energy for the sec-butyl carbonium ion is strongly negative, therefore, this process is highly favored even in a model of thermally treated γ-Al_2O_3 (see Figs. 5 and 6). The sulfated-alumina shows highly negative values for this carbonium formation (see Table 4).
2. The carbanionic mechanism for double-bond isomerization can take place when Lewis basic sites are present on γ-Al_2O_3 (Figs. 5 and 6).

Obviously, the presence of sulfate groups or halogen groups decreases drastically the concentration of these sites [2]. It is clear that the *cis/trans* ratio achieves the values near to equilibrium, being *trans*-2-butene favored (reactions 4–7). If the formation of sec-butyl cation takes place on weak BA sites at low reaction temperatures, the *cis*-2-butene would be preferred by steric reasons (Scheme 2). The Lewis basic sites seem to be active at high reaction temperature [2].

3. The skeletal isomerization to isobutene by a monomolecular mechanism is very favored through the formation of a tert-butyl carbonium (reactions 9 and 10). Desorption of isobutene is a difficult process (reactions 10 and 11), even in presence of 1-butene on pure alumina. This fact explains why we need high temperatures to obtain isobutene formation and the probability of catalytic deactivation by strong coordination of adsorbed species if the reaction is done at low temperatures. The presence of sulfur seems to make the isobutene desorption process easier (reaction 13). At low temperatures desorption of *cis/trans*-2-butene would be preferred as a global reaction. Remember that we are using these energy changes as changes in the total Gibbs energy when no intermediates are involved. The steric reasons could be responsible for the higher initial *cis/trans* ratio at low temperatures (Scheme 2 and reactions 14 and 15).

4. If enough acidic sites are considered and we analyze the probability of dimerization reactions, we can visualize that the formation of octenyl carbonium is favored at high butene pressures, if the sec-butyl cation life time on the catalyst is long enough and the bond is strong (reactions 16–18). Energy difference between reaction 16 (Table 7) and reaction 9 (Table 6) is near −2.1 eV favoring reaction 16. The bimolecular mechanism to obtain isobutene is strongly suppressed at high temperatures. This behavior could be related to the lifetime of the carbocation [8]. The steric requirements for this reaction to take place are clear. In this sense, the presence of the LA sites could be important.

5. Desorption of cracked by-products (propylene, pentene) is difficult (see reactions 19 and 20). This mechanism is an alternative for isobutene and double-bond isomerization reactions (reactions 21–24). The steric requirements for further oligomerization are important to be considered, especially if we have high SO_x coverage.

References

[1] J.W. Ward, in: B.E. Leach (Ed.), Applied Industrial Catalysis, Vol. 3, Academic Press, Orlando, 1981, p. 272.

[2] K. Tanabe, M. Misono, Y. Ono, H. Hattori, New Solid Acids and Bases, Kodansha, Tokyo; Studies in Surface Science and Catalysis, Vol. 51, Elsevier, Amsterdam, 1986.

[3] Z.-X. Cheng, V. Ponec, Catal. Lett. 27 (1994) 113.

[4] P. Nortier, P. Fourre, A.B. Mohammed Saad, O. Sauer, J.C. Lavalley, Appl. Catal. 61 (1990) 141.

[5] D.S. Mener, W.H. Wilmot, J.M. Bridges, J. Catal. 3 (1964) 502.

[6] Z.-X. Cheng, V. Ponec, J. Catal. 143 (1994) 607.

[7] J. Hounvicka, V. Ponec, Catal.-Rev. Sci. Eng. 39 (1997) 319.

[8] J. Hounvicka, O. Diefenbach, V. Ponec, J. Catal. 164 (1996) 288.

[9] O. Ramis, P.F. Rossi, O. Busca, V. Lorenzelli, Langmuir 5 (1989) 917.

[10] J. Hounvicka, V. Ponec, Appl. Catal. A 145 (1996) 95.

[11] L.H. Gielgens, I.H.E.. Veenstra, V. Ponec, M.J. Haanepen, J.H.C. Van Hoof, Catal. Lett. 32 (1995) 195.

[12] M. Simon, S.L. Suib, C.L. O'Young, J. Catal. 147 (1994) 484.

[13] W.-Q. Xu, Y.-G. Yin, S.L. Suib, C.-L. O'Young, J. Catal. 163 (1996) 232.

[14] M. Asensi, A. Corma, A. Martinez, J. Catal. 158 (1996) 561.

[15] J. Hounvicka, V. Ponec, Ind. Eng. Chem. Res. 36 (1997) 1424.

[16] Z.-X. Cheng, V. Ponec, Appl. Catal. A 118 (1994) 127.

[17] J.B. Peri, Phys. Chem. 69 (1965) 220.

[18] H. Knözinger, C.P. Kaerlein, J. Catal. 25 (1972) 436.

[19] W. Pryzystajko, R. Fiedorow, I.G. Dalla Lana, Appl. Catal. 15 (1985) 265.

[20] P. Patrono, A. La Ginestra, G. Rainis, G. Busca, Appl. Catal. A 107 (1994) 249.

[21] T. Yamaguchi, T. Jin, T. Ishida, K. Kanabe, Mat. Chem. Phys. 17 (1987) 3.

[22] T. Yamaguchi, Appl. Catal. 61 (1990) 1.

[23] K. Arata, M. Hino, Appl. Catal. 59 (1990) 197.

[24] J. Engelhardt, G. Onyestyák, W.K. Hall, J. Catal. 157 (1995) 721.

[25] H.R. Gerberich, F.E. Lutinski, W.K. Hall, J. Catal. 6 (1966) 209.

[26] H. Knözinger, P. Ratnasamy, Catal.-Rev. Sci. Eng. 17 (1978) 31.

[27] A.K. Ohosh, R.A. Kydd, Catal.-Rev. Sci. Eng. 27 (1985) 359.

[28] A. Corma, V. Fome, F. Melo, Appl. Catal. 61 (1990) 175.

[29] E.C. DeCanio, J.W. Bruno, V.P. Nero, J.C. Edwards, J. Catal. 140 (1993) 84.

[30] G.B. Mavicher, C.J. Kim, J.J. Eggert, J. Catal. 80 (1983) 315.

[31] L. Gielgens, M. Van Kampen, M. Broek, R. Van Hardeveld, V. Ponec, J. Catal. 154 (1995) 201.

[32] S.S. Meijers, L. Gielgens, V. Ponec, J. Catal. 156 (1995) 147.

[33] V. Logie, G. Maire, D. Michel, J. Vignes, J. Catal. 188 (1999) 90.

[34] M. Hino, K. Arata, J. Chem. Soc., Chem. Commun. 851 (1980).

[35] R. Hofmann, J. Chem. Phys. 39 (1963) 1392.

[36] I. Chamber, L. Forrs, G. Calzaferri, J. Phys. Chem. 93 (1989) 5366.

[37] M.L. Ferreira, M. Volpe, J. Mol. Cat. A: Chem. 149 (1999) 33–42.

[38] M.L. Ferreira, D. Damiani, A. Juan, Comput. Mat. Sci. 9 (1998) 357.

[39] C. Pisani, M. Causa, R. Dovesi, C. Roetti, Prog. Int. Surf. Sci. 25 (1987) 119.

[40] S. Wilson, J. Mc Connell, J. Phys. Chem. 34 (1980) 315.

[41] H. Könizinger, X. Ratnasamy, Catal. Rev. 17 (1978) 31.

[42] T. Shay, L.-Y. Hsu, J.M. Basset, Sh. Shore, J. Mol. Catal. 86 (1994) 479.

[43] D.E. Galindo, M.J. Goncalves, M.M. Ramirez-Corredores, in: A. Corma, F.V. Melo, S. Mendioroz, J.L.G. Fierro (Eds.), Studies in Surface Science and Catalysis, Vol. 130, 2000, pp. 1205.